Sensors and Materials, Vol. 34, No. 5 (2022) 1927–1941
MYU Tokyo

S & M 2943

Design and Implementation of Tandem Container Weigh-in-motion System Based on Radial Basis Function Neural Network

Zhong-Jie Liu,[1] Che-Wen Chen,[2] and Shih-Pang Tseng[1,3*]

[1]School of Software, Changzhou College of Information Technology,
No. 22, Mingxin Middle Road, Changzhou, Jiangsu 213164, China
[2]Department of Electrical Engineering, National Cheng Kung University,
No.1, University Road, Tainan City 701, Taiwan (R.O.C)
[3]School of Information Science and Technology, Sanda University,
No. 2727 Jinhai Road, Pudong District, Shanghai 201209, China

(Received June 30, 2021; accepted May 9, 2022)

Keywords: logistics, weigh-in-motion, RBF neural network

Weigh-in-motion (WIM) systems are designed to capture and record vehicle weights when a vehicle directly passes the WIM measurement region in a normal speed range. WIM systems make the weighing process more efficient than the static weighing system. At present, most types of transportation use containers in international trade. Therefore, in this paper, we propose a novel design of a WIM system for tandem containers, and the radial basis function (RBF) neural network (NN) is used to enhance the accuracy of the weighing result. First, we briefly introduced the hardware structure and the system model of WIM. Next, we used the RBF NN to simulate the WIM model and proposed a self-adaptive algorithm for the center of gravity shifting. The WIM software system was implemented, and the experimental results showed that the error of this system was less than 3%.

1. Introduction

With the vigorous development of international trade, container transportation is playing an increasingly important role in international shipping owing to its high efficiency, safety, and convenience. While the use of containers to transport bulk goods is favored by people, transportation safety has also been put on the agenda. To ensure transportation safety, the weight of each container must not exceed the specified weight. Currently, ports generally use the following three methods to weigh tandem container vehicles:(1) the first is to use a special hoisting scale to weigh them in stages, which is costly and low in efficiency; the second is to use a static weighing method to evenly distribute the weight after the total weight is determined by a truck scale. The unevenness of the cargo during the loading of the container causes the center of gravity to deviate. Therefore, not only is the single-box weighing inaccurate, but also overweight boxes cannot be detected and banned.

The third is to use dynamic axle weighing to measure the weight of the vehicle axle, because the sensor is accompanied by the generation of various axle load interference signals and the

*Corresponding author: e-mail: tsengshihpang@czcit.edu.cn
https://doi.org/10.18494/SAM3496

ISSN 0914-4935

adaptation of the vehicle speed range is small. Therefore, the measurement accuracy is low, and it is difficult to popularize the dynamic axle weighing. For this problem of weighing a single container of vehicles in tandem containers, we propose a dynamic single-container weighing system for vehicles based on tandem containers. On the basis of the construction of the dynamic weighing model, the radial basis function (RBF) neural network (RBFNN) is applied to improve the weighing accuracy. An adaptive correction algorithm is established for the deviation of the cargo center of gravity. On the other hand, a set of dynamic weighing system software modules are developed to improve the efficiency of harbor container weighing.

The remainder of this paper is organized as follows. The related works are presented in Sect. 2. In Sect. 3, we briefly introduce the prototype system. The proposed adaptive algorithm is described in detail in Sect. 4. In Sect. 5, we demonstrate the implementation of the prototype system. The conclusions are given in Sect. 6.

2. Related Work

2.1 Dynamic weighing system

In recent years, a large number of dynamic weighing systems have been developed, including the American high-speed dynamic weighing instrument, the static and dynamic vehicle weighing system of PEEK UK, the road weight toll system of Singapore Hyde International Group, the weighing toll system developed by Beijing Zhongshan Research Institute Weighing Instrument Factory, the SM2000s dynamic weighing system developed by Zhongshan Highway Automation Equipment Co., Ltd., and the fixed dynamic vehicle weighing system of Chongqing Highway Research Institute of the Ministry of Communications, China.

The truck scale dynamic weighing system can considerably improve the efficiency of the logistics.[2,3] However, weighing error is the key factor of the dynamic weighing system, in which it is important to reduce the error to an acceptable level and to allow a higher speed limit of the truck.

In 2015, Dong *et al.*[4] proposed a dynamic truck scale weighing system for containers. It simply used three weighing platforms to reduce the error. They focused on reducing the effect of low-frequency vibration due to the passing of the truck on the weighing system. However, there are some limitations. First, this system needs to have the static data of the truck models beforehand. The second is that it allows only one container on the truck.

In 2015, Zhang *et al.*[5] proposed a vehicle dynamic weighing algorithm based on a double-weighing platform truck scale. First, it uses wavelet transformation to filter a weighing signal. An expert system is used to identify the vehicle type and the speed of the axle to calculate its acceleration. In this work, the BP network is constructed according to the weighing signal, speed, acceleration, and axle type of the vehicle. It uses the self-learning ability of the BP network and trains a large amount of data to achieve higher dynamic weighing precision.

In 2020, Lai *et al.*[6] proposed to analyze the various factors that affect the static performance, such as sensor and platform tilt installations. These factors will affect the static and dynamic weighing accuracies. The dynamic truck scale weighing system with or without static calibration

is used in the test process. The results show that the dynamic performance index can meet the requirements only after the static calibration is used.

2.2 Deep learning

A standard neural network (NN) consists of many simple, connected neurons that can produce a sequence of real-valued calculations and activations.[7–9] These neurons are well organized and divided by three or more layers. In the first layer, also denoted by input layers, neurons receive outside inputs. The other neurons become activated through weighted connections from active neurons of the previous layer. Learning is achieved by adjusting the weights between the neurons of the neighboring layers in order to obtain the NN with the expected behavior and performance. The term "Deep Learning"[10] is used to describe these developments in the new millennium and driven by computing power.

The RBFNN[11,12] is a type of artificial NN that uses RBFs as activation functions of the neurons. The linear combination of RBFs is applied to the output layer. The RBFNN has been successfully used in various applications, such as classification,[13,14] system control,[15–17] and battery aging assessment.[18]

3. Proposed System

3.1 Model of proposed system

In this paper, the proposed weighing platforms are mainly composed of dynamic axle load truck scale, static truck scale, dynamic detection instrument, static detection instrument, data acquisition device, LCD display, printer, workstation, and signal indicator, as shown in Fig. 1. When the vehicle to be tested passes through the weighing platform at a uniform speed of 5–15 km/h, the dynamic weighing instrument measures the weight of the front, middle, and rear axles of the vehicle, and the static weighing instrument measures the total weight of the vehicle.

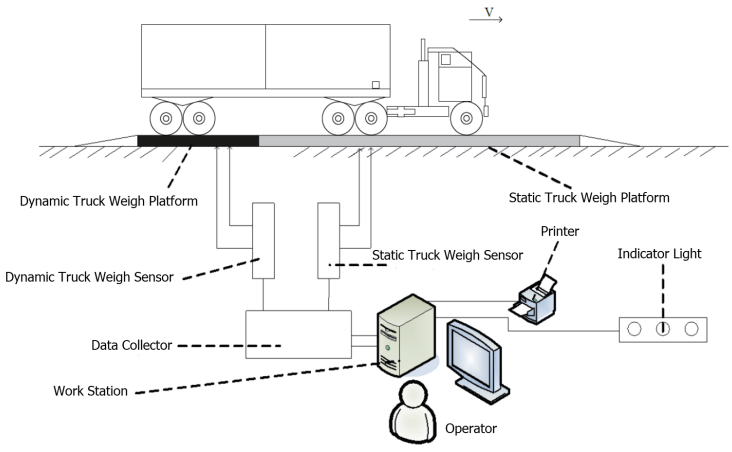

Fig. 1. (Color online) Architecture of weighing platform.

Owing to the difference in measurement accuracy between the dynamic axle load truck scale and the static total weight scale, the least square error method is used to calculate the weight ratio coefficient, and the measured static and dynamic total weights are determined and subtracted from the total weight of the unloaded vehicle to obtain the total weight of the cargo and then to calculate the center of gravity offset along the length, the weight of the front container, and the weight of the rear container through the RFBNN.

The hardware structure of the data acquisition device in the weighing platform mainly includes a pressure sensor, an acceleration sensor, a signal amplification and bias circuit, a forward channel formed by an A/D converter, and a wireless data interface. The STM32F1032E SoC is the core part that includes the program memory, data memory, and additional program memory. When the vehicle under test passes the weighing platform, the load cell and acceleration sensor convert the weight value and vibration quantity into analog electrical signals, send them to the analog input terminal of the A/D converter through the amplifier, and then convert them to digital signals for processing. The processing result is sent to the LCD as a dynamic measurement weight, and the data are sent to the printer for printing. The data can also be sent to the computer through the switch and RS-232 level converter for storage or further processing, as shown in Fig. 2.

Owing to the difference in vehicle type, each vehicle is simplified to only one support shaft to make the calculation method easy and widely used. The simplified diagram of the actual force state of the tandem container vehicle is shown in Fig. 3.

On the basis of the principle of force and moment balance, we can derive Eqs. (1) and (2) if there are n support shafts under each car.

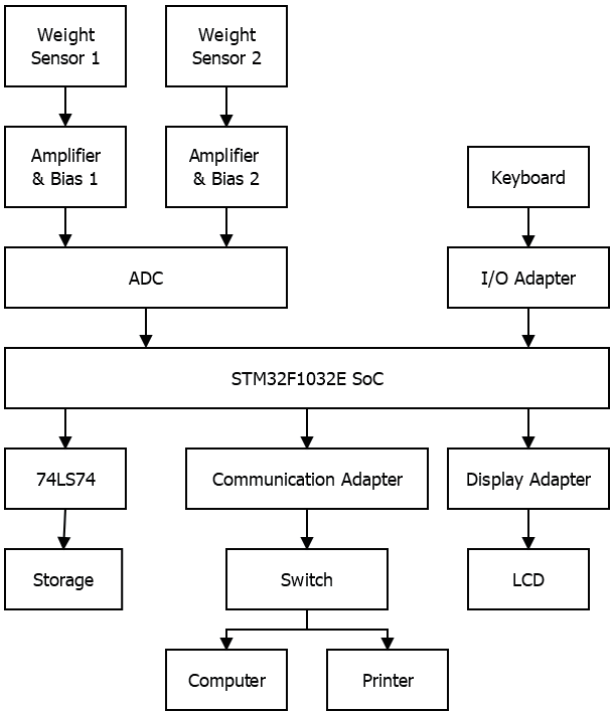

Fig. 2. Model of weighing platform.

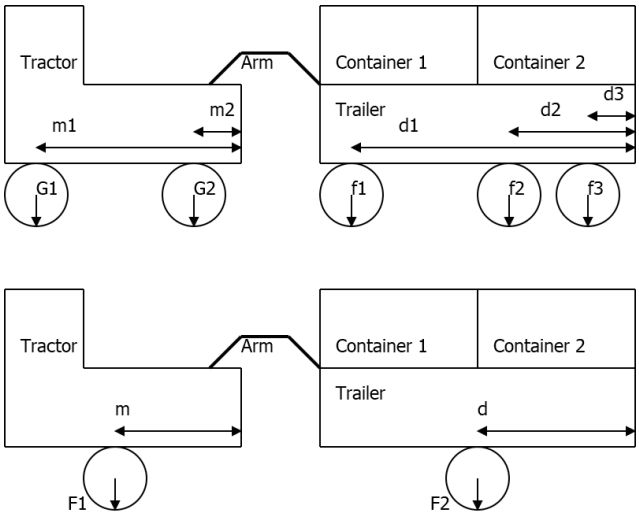

Fig. 3. Simplified actual force state of tandem container vehicle.

$$F = f_1 + f_2 + f_3 + \cdots + f_n \tag{1}$$

$$l = \frac{f_1 \times d_1 + f_2 \times d_2 + f_3 \times d_3 + \cdots + f_n \times d_n}{f_1 + f_2 + f_3 + \cdots + f_n} \tag{2}$$

3.2 Estimating the weighing model of ideal cases

When this assumption is made, if the loading vehicle runs at speed v when weighing, and there are multiple support shafts under a certain section of the loading vehicle, the shortest distance between any two adjacent shafts is S. To ensure that the dynamic axle load truck scale accurately measures the pressure on each bearing, it requires each weighing time $t \le \frac{S}{v}$.

When the whole vehicle runs at a constant speed, the total dynamic friction force against the ground is f_T. The coefficient of friction is denoted as μ and the total weight of the entire system can be obtained as G_T, as shown in Eqs. (3) and (4). The total weight of the containers, $G_{containers}$, can be calculated using Eq. (5).

$$\frac{f_T}{\mu_T} = G_T \tag{3}$$

$$G_T = G_{Tractor} + G_{Trailer} + G_{containers} \tag{4}$$

$$G_{containers} = G_{container1} + G_{container2} = \frac{f_T}{\mu_T} - G_{Tractor} - G_{Trailer} \tag{5}$$

When the vehicle is running at a constant speed, it is ideally assumed that the cargo in the container is evenly distributed, that is, the center of gravity of the container is at the center of its position. The simplified contact point between the tire and the trailer is used as the support point. The distance between the support point and the rear of the vehicle is l, and the length of the container is L, and it is assumed that the centers of gravity of the containers are in the respective centers of the containers. The direction of the lever arm of the trailer supported by the vertical upward direction of the tractor is away from the rear of the trailer, that is, the distance between the center pin and the rear of the trailer is L_3, and the actual center of gravity of the trailer away from the support point is $L_{trailer}$. The force on the tractor and the balance analysis of the trailer torque are shown in Fig. 4.

According to the torque balance shown as Eq. (5), we can determine the weight of each container using Eqs. (6) and (7).

$$G_{container1} \times (\tfrac{3}{2}L - l) + G_{container2} \times (\tfrac{1}{2}L - l) + G_{trailer} \times l_{trailer} = F \times (l_3 - l) \tag{6}$$

$$G_{container1} = \frac{G_{trailer} \times (\frac{1}{2}L - l - l_{trailer}) + G_{tractor} \times (\frac{1}{2}L - l_3) + \frac{f_1}{\mu_1} \times (l_3 - \frac{1}{2}L) + \frac{f_2}{\mu_2} \times (l - \frac{1}{2}L)}{L} \tag{7}$$

$$G_{container2} = \frac{G_{trailer} \times (l_{trailer} + l - \frac{3}{2}L) + G_{tractor} \times (l_3 - \frac{3}{2}L) + \frac{f_1}{\mu_1} \times (\frac{3}{2}L - l_3) + \frac{f_2}{\mu_2} (\frac{3}{2}L - l)}{L} \tag{8}$$

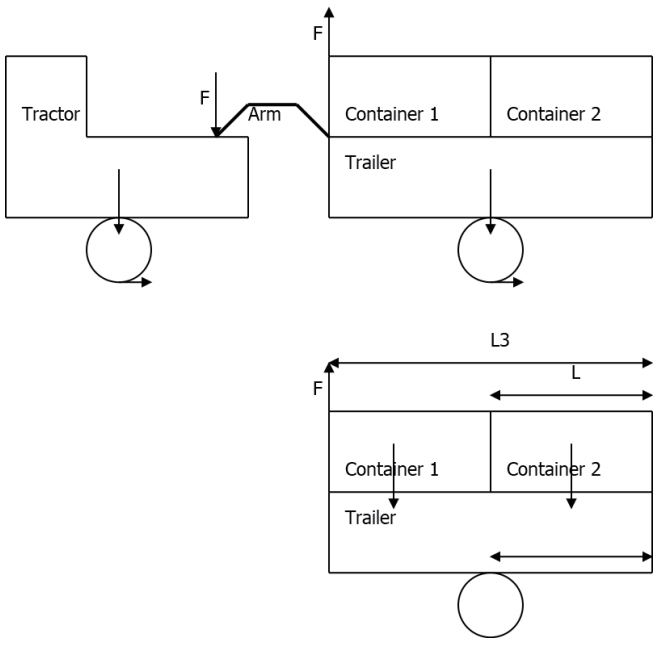

Fig. 4. Torque balance analysis of tractor and trailer.

Here, the physical quantities that need to be known are the weight of the trailer ($G_{trailer}$), the weight of the tractor ($G_{tractor}$), the dynamic friction (f_1) and friction coefficient (μ_1) of the trailer, the dynamic friction (f_2) and friction coefficient (μ_2) of the tractor, and the length of the container (L). The distance between the support point of the tractor and the rear of the vehicle is l. The distance between the center pin and the tail of the trailer is l_3, and the displacement of the actual center of gravity of the trailer from the support point is $l_{trailer}$.

Finally, $l_{trailer}$ is estimated by using the data of the vehicle when it is empty, as shown in Fig. 5. When the loading vehicle is empty, let the ground pressure of the tractor be F_{10}, the ground pressure of the trailer be F_{20}, and the vertical upward support force of the tractor on the trailer be F_0; thus, we can determine the ground pressure as

$$F_{10} = F_0 + G_{trailer}. \tag{9}$$

Then, we take the simplified contact point between the tire and the trailer as the support point to take the moment, and we can derive the following equations:

$$G_{trailer} \times l_{trailer} = F_0 \times (l_3 - l), \tag{10}$$

$$l_{trailer} = \frac{(F_{10} - G_{trailer}) \times (l_3 - l)}{G_{trailer}}. \tag{11}$$

We substitute these equations into Eqs. (7) and (8), and since the actual measured value is equal to the pressure of the tractor tire, the actual measured value is equal to the pressure of the trailer tire. Moreover, the pressure of the tire can be dynamically measured as

$$G_{Container1} = \frac{G_{Trailer} \times (\frac{1}{2}L - l) + G_{Tractor} \times (\frac{1}{2}L - l) + F_1 \times (l_3 - \frac{1}{2}L) + F_2 \times (l - \frac{1}{2}L) - F_{10} \times (l_3 - l)}{L}, \tag{12}$$

$$G_{Container2} = \frac{G_{Trailer} \times (l - \frac{3}{2}L) + G_{Tractor} \times (l - \frac{3}{2}L) + F_1 \times (\frac{3}{2}L - l_3) + F_2 \times (\frac{3}{2}L - l) + F_{10} \times (l_3 - l)}{L}. \tag{13}$$

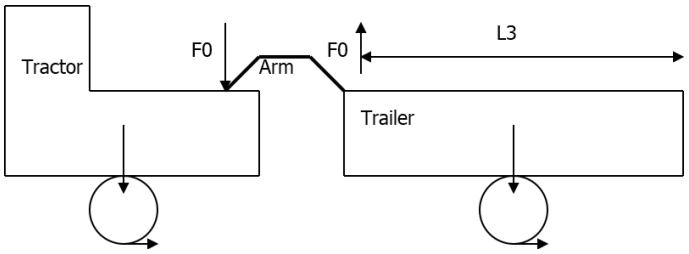

Fig. 5. Analysis of empty load.

Here, the physical quantities that need to be known are the total pressure of the tractor against the ground (F_1), the total pressure of the tractor against the ground (F_2), and the total pressure of the tractor against the ground when the tractor is empty (F_{10}). The distance between the support point of the tractor and the rear of the vehicle is l, which is related to the position distribution and the number of support shafts, n, under the trailer of the loading vehicle in practical situations.

3.3 Estimating the weighing model of ideal cases

In actual transportation, owing to different goods being transported, the physical center of gravity of the container is not at its center of gravity. Assuming that the contact point between the tire and the trailer is the support point, the distance between the support point and the rear of the trailer is l, the actual center of gravity of the trailer is away from the support point, and the distance between the center pin and the rear of the trailer is $l_{trailer}$. Let the actual physical center of gravity of container 1 be the distance from the rear of the vehicle, and the actual physical center of gravity of container 2 shall be the distance from the rear of the vehicle. As shown in Fig. 6, it is necessary to perform a torque analysis on the trailer in this case. According to the torque balance, we can derive

$$G_{container1} \times (x_1 - l) + G_{container2} \times (x_2 - l) + G_{trailer} \times l_{trailer} = F \times (l_3 - l). \tag{14}$$

Then, the weight of each container can be calculated as

$$G_{container1} = \frac{G_{tractor} \times (x_2 - l) - G_{trailer} \times (l - x_2) + F_1 \times (l_3 - x_2) - F_2 \times (x_2 - l) - F_{10} \times (l_3 - l)}{x_1 - x_2}, \tag{15}$$

$$G_{container2} = \frac{G_{tractor} \times (l - x_1) + G_{trailer} \times (l - x_1) + F_1 \times (x_1 - l_3) + F_2 \times (x_1 - l) + F_{10} \times (l_3 - l)}{x_1 - x_2}. \tag{16}$$

Here, x_1 and x_2 are the distances from the rear of the trailer to the real gravity center of containers

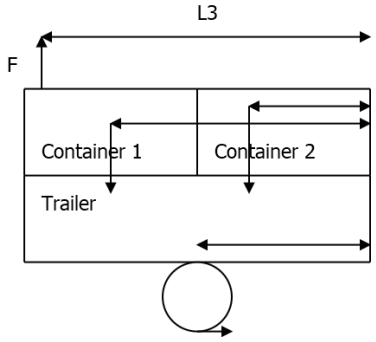

Fig. 6. Analysis of trailer with real load.

1 and 2 with loads, respectively. They are also the critical factors that affect the estimation of the weight of containers. In the dynamic weighing process, it is not practical to measure the real position of the center of gravity of the containers. If we assume the center of gravity of the container with loads near the geometric center of the container, the difference between the center of gravity and the geometric center will lead to a large error. This is not acceptable in many real applications, and the container loading process cannot ensure that the real position of the center of gravity should be near the geometric center. In this study, we proposed an approach based on the RBFNN to estimate the center of gravity of the container to reduce the error of the dynamic weighing process.

In summary, this system intends to use the relationship between the dynamic equilibrium conditions of the vehicle in motion and the pressure and friction to establish a mathematical model of the cargo center of gravity position L_1' along the length of the container, shown as

$$L_1' = \left(\sum_{i=1}^{n} M_i'' \right) / G, \tag{17}$$

where G is the total weight of the cargo. When the two containers of the cargo are regarded as a whole, M_i'' is the moment centered on the simplified force system of the trailer. The mathematic model of the weight of the front container is shown as

$$G_1 = \left(\sum_{i=1}^{n} M_i \right) / L. \tag{18}$$

The mathematical model of the weight of the rear container is shown as

$$G_2 = \left(\sum_{i=1}^{n} M_i' \right) / L. \tag{19}$$

4. Adaptive Algorithm

In the traditional static weighing system, the vehicle speed is zero in the weighing process. On the other hand, the vehicle speed is not a constant in the dynamic weighing system. The momentum and vibration affect the measurement accuracy. Therefore, an adaptive algorithm is needed to compensate for the effects of the momentum and vibration within a certain vehicle speed range. In this study, we chose the RBFNN as the adaptive algorithm to control the measurement error in the proposed dynamic weighing system.

4.1 Model of algorithm

The RBFNN is a typical three-layer forward NN. The most basic RBFNN includes three layers, namely, the input layer, the hidden layer (middle layer), and the output layer.[10,11] The

input layer is composed of some source points (perception units) that connect the network with the external environment and only play a role in the transmission of data information, without any transformation of input information; the kernel function (or function of the hidden layer neuron) is taken as the RBF, which performs a nonlinear transformation between the input information and the hidden layer space, and usually has a higher dimensionality; the output layer is linear and provides a response to the activation mode of the input layer.[12] The topological structure is shown in Fig. 7.

The numbers of neurons on the input, hidden, and output layers are N, M, and P, respectively. The input pattern is denoted as $X = [x_1, x_2, \ldots, x_n]$ and the output pattern is denoted as $Y = [y_1, y_2, \ldots, y_p]$. In this paper, the Gauss RBF is the hidden layer node and the hidden unit output is obtained as

$$\Phi_j = \exp\left(-\left\|\frac{X - C_j}{\sigma_j}\right\|^2\right), \tag{20}$$

where $j = 1, 2, \ldots, m$ and Φ_j is the output of the j-th neuron in the hidden layer. $\|\cdot\|$ is the Euclidean norm and C_j and σ_j are the center and width of the hidden neuron j, respectively. C_j is also the input vector of the j-th neuron in the hidden layer, $C_j = [x_{j1}, x_{j2}, \ldots, x_{jn}]$.

The input and output relationship expression of the output layer neuron is

$$y_k = \sum_{j=1}^{M} w_{kj} \Phi_j, \tag{21}$$

where $k = 1, 2, \ldots, p$ and y_k is the output of the j-th neuron in the output layer, and w_{kj} is the weight between the j-th neuron in the hidden layer and the k-th neuron in the hidden layer.

4.2 Design of algorithm

This system uses the Gauss RBF as the hidden node to construct a multi-input dual-output RBF three-layer forward feedback network model, that is, the nonlinear function is the Gauss

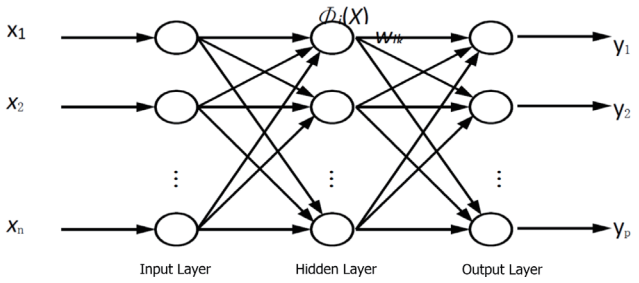

Fig. 7. RBF network.

RBF. The width σ and the weight W are used to adjust the algorithm. The neurons in the hidden layer are selected according to the empirical formula

$$h = \sqrt{m+n} + a, \tag{22}$$

where m is the number of input nodes, n is the number of output nodes, and the constant a is between 0 and 10. The adaptive adjustment is via the sample training, the K-means clustering algorithm is used to determine the center of the hidden layer RBF, and the width is calculated as

$$\sigma = \frac{d_{max}}{\sqrt{2h}}, \tag{23}$$

where d_{max} is the maximum distance between the centers of the basis functions obtained by the K-means clustering algorithm. h is the number of neurons on the hidden layer. The K-means clustering algorithm mainly performs the mapping calculation of the neural unit from the input layer to the hidden layer. This clustering algorithm is a basic division method in the clustering method, and the sum of square error criterion functions is often used as the clustering criterion function.

In the weight update process, the recursive least squares (RLS) algorithm has a higher convergence rate than the traditional gradient descent algorithm, and it can solve the linear optimization problem of the connection weight between the hidden layer and the output layer.

The numbers of neurons in the input, hidden, and output layers of the RBFNN are 7, 8, and 2, respectively, the maximum number of cycles is 20, and the training error is 3%. The key neuron factors in the RBFNN model are the front axle load F_1, middle axle load F_2, rear axle load F_3, vehicle speed V, included angle θ, the distance between traction axles and trailers, d_1, distances between the axle and the tail of the trailers, d_2 and d_3, the distance between the center pin and the tail of the trailer, l_3, the weight of the unloaded tractor, T_1, the weight of the unloaded trailer, T_2, the ground pressure of the unloaded tractor F_{10}, container length L, maximum rated load δ, the mass center of gravity of the trailer, G, and the distance between the center of gravity of the trailer and the front of the container, L_1. The real weights of the front and rear boxes are mainly used to control the degree of convergence of the iteration, that is, after the iteration end condition is met, the result is automatically saved and the calculation is terminated. After substituting a large number of experimental samples for network training, it is found that when the number of training samples increases to 20, the training error meets the target requirement of less than or equal to 3%, and the training can be stopped. The simulation effect is shown in Fig. 8.

5. Performance Analysis

In this paper, three different models, namely, FAW Jiefang CA4222P21K2T3A1E, FAW Jiefang CA4252P21K2T1A2E, and FAW Aowei CA4252P21K2T1E are tested in actual tests. The specific parameter data are collected in Changzhou Hongshida Electric Manufacturing Co., Ltd.

When a double-container vehicle loaded with real objects is traveling at a constant speed of 5–15 km/h on an over-dynamic static joint weighing platform, the movement state is recorded in turn when passing through the dynamic axle weighing platform. We download the front axle load F_1, middle axle load F_2, and rear axle load F_3 of the freight vehicle, and through the management recognition software, we determine the best output correction value of the vehicle to be tested and measure the dynamic total weight $G_{dynamic}$, as shown in Table 1.

The static total weight G_{static} is recorded through the static weighing platform. Using the management recognition software, the corrected axle weight P'n and the corrected G_{static} are measured, as shown in Table 2.

To facilitate the promotion and application of the algorithm proposed in this paper, the algorithm is specially packaged as a dynamic link library, and a set of dynamic single-box weighing software systems for serial containers has been developed. The development environment of the software system is Visual Studio 2010, the database is SQL Server 2008, and the software interface is shown in Fig. 9.

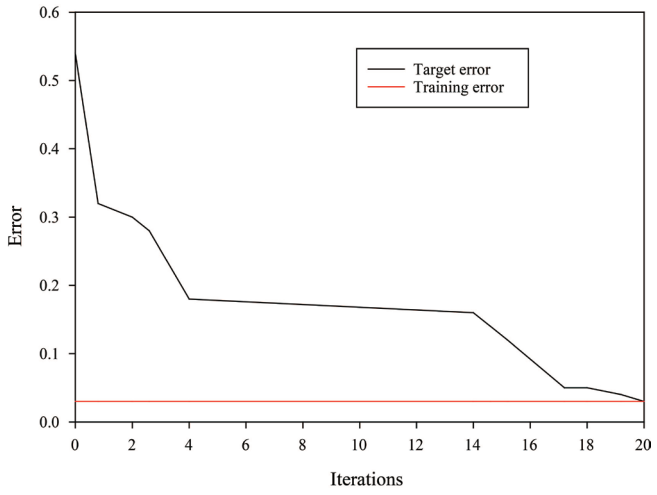

Fig. 8. (Color online) RBFNN training error number of iterations.

Table 1
Results of dynamic weighing.

	Jiefang CA4222P21K2T3A1E	Jiefang CA4252P21K2T1A2E	Aowei CA4252P21K2T1E
Speed v_1 (km/t)	4.890	4.890	4.890
Speed v_2 (km/t)	5.120	5.120	5.120
Speed v_3 (km/t)	9.870	9.870	9.870
Speed v_4 (km/t)	10.14	10.14	10.14
Speed v_5 (km/t)	14.56	14.56	14.56
Front axle F_1 (kg)	4775.56	5765.23	3664.21
Middle axle F_2 (kg)	12625.14	20425.23	27312.35
Rear axle F_3 (kg)	37520.98	29254.35	38736.21
$G_{dynamic}$ (kg)	43561.45	55444.81	69712.17

Table 2
Results of static weighing.

	Jiefang CA4222P21K2T3A1E	Jiefang CA4252P21K2T1A2E	Aowei CA4252P21K2T1E
Total weight (empty) T (kg)	16080	14780	17080
Front axle (empty) P'_1 (kg)	4360	4240	3680
Middle axle (empty) P'_2 (kg)	5900	6480	6500
Rear axle (empty) P'_3 (kg)	5500	6020	6100
Container A length L_A (mm)	6058	6058	6058
Container A weight (empty) G_A' (kg)	1600	1600	1600
Container B length L_B (mm)	6058	6058	6058
Container B weight (empty) G_B' (kg)	1700	1700	1700
Arm length d (mm)	7645	6425	5876
Shift for center of gravity Δd_A (mm)	300	200	300
Shift for center of gravity Δd_B (mm)	200	200	100
Correction factor $K = G_{sta}/G_{dyn}$	1.2611	0.9991	1.0282
G_{static} (kg)	54938	55400	71680

Fig. 9. (Color online) User interface of system.

6. Conclusions

The dynamic single-box weighing system based on tandem containers proposed in this paper can effectively improve the accuracy of single-box dynamic measurement and can meet the error accuracy control within 3%. This system can meet the requirements of port container dynamic single-box overweight detection. In the future, a variety of sensors will be used to transform the

static and dynamic weighing platforms to enhance the detection capability of the system when the vehicle is traveling at a high speed, further improve the efficiency and accuracy of dynamic container weighing, and reduce the cost of dynamic container weighing.

Acknowledgments

This work was supported by Excellent Young Key Teachers of Jiangsu University "Qing Lan Project" in 2020, the Research Project of Jiangsu Higher Education Reform in 2019 "Theoretical and Practical Research on the Construction of High-level Professional Clusters under the Background of 'Double Heights'" under Grant No. 2019JSJG431, and the Teaching Innovation Team of Changzhou College of Information Technology.

References

1 X. Fang, Z. Ji, Z. Chen, W. Chen, C. Cao, and J. Gan: Sustainability **12** (2020) 1487. https://doi.org/10.3390/su12041487
2 Z. Zhou: Proc. AASRI Winter Int. Conf. Engineering and Technology (AASRI-WIET, 2013) 170.
3 M. Mangeas, S. Glaser, and V. Dolcemascolo: Proc. 5th Int. Conf. Information Fusion 2002 (IEEE Fusion, 2002) 456.
4 M. Dong, F. Zhu, and W. Yu: Proc. 1st Int. Conf. Information Science, Machinery, Materials and Energy (2015). https://doi.org/10.2991/icismme-15.2015.21
5 X.-D. Zhang, L.-H. Li, and Y.-G. Song: Transducer Microsyst. Technol. **6** (2015) 133.
6 Z. Lai, X. Yang, and J.-H. Yao: ACTA IMEKO **9** (2020) 69. https://doi.org/10.21014/acta_imeko.v9i5.941
7 S. Smys, J. I. Z. Chen, and S. Shakya: J. Soft Comput. Paradigm **2** (2020) 186. https://doi.org/10.36548/jscp.2020.3.007
8 W. Liu, Z. Wang, X. Liu, N. Zeng, Y. Liu, and F. E. Alsaadi: Neurocomputing **234** (2017) 11. https://doi.org/10.1016/j.neucom.2016.12.038
9 A. Bashar: J. Artif. Intell. Capsule Networks **1** (2019) 73. https://doi.org/10.36548/jaicn.2019.2.003
10 J. Schmidhuber: Neural Networks **61** (2015) 85. https://doi.org/10.1016/j.neunet.2014.09.003
11 Y. Lu, N. Sundararajan, and P. Saratchandran: IEEE Trans. Neural Networks **9** (1998) 308. https://doi.org/10.1109/72.661125
12 F. Schwenker, H. A. Kestler, and G. Palm: Neural Networks **14** (2001) 439. https://doi.org/10.1016/S0893-6080(01)00027-2
13 R. Erol, S. N. Oğulata, C. Şahin, and Z. N. Alparslan: J. Med. Syst. **32** (2008) 215. https://doi.org/10.1007/s10916-007-9125-5
14 S. S. Chouhan, A. Kaul, U. P. Singh, and S. Jain: IEEE Access **6** (2018) 8852. https://doi.org/10.1109/ACCESS.2018.2800685
15 C.-C. Wei and L.-C. Hung: Proc. 2020 IEEE 8th Int. Conf. Orange Technologies (IEEE ICOT, 2020). https://doi.org/10.1109/ICOT51877.2020.9468718
16 C.-C. Wei, B. Qin, L.-C. Hung, C.-W. Chen, and S.-P. Tseng: 2020 IEEE 8th Int. Conf. Orange Technologies (IEEE ICOT, 2020). https://doi.org/10.1109/ICOT51877.2020.9468795
17 R. Sitharthan, P. Thirumanickam, S. Rani.S, and K. C. Ramya: Trans. Inst. Meas. Control **41** (2019) 3158. https://doi.org/10.1177/0142331218823858
18 C. She, Z. Wang, F. Sun, P. Liu, and L. Zhang: IEEE Trans. Ind. Inf. **16** (2020) 3345. https://doi.org/10.1109/TII.2019.2951843

About the Authors

Zhong-Jie Liu received his B.S. degree from Xinyang Normal University in 2006 and his M.E. degree from Changzhou University in 2010. From 2010 to 2015, he worked in Changzhou Institute of Advanced Manufacturing Technology and engaged in intelligent control systems, software architecture design, and image recognition and other fields of research and development. In 2015, he joined Changzhou College of Information Technology. He had guided students many times to win the first prize in national and provincial competitions, and won the first prize in the Software Cup National Competition for two consecutive times. In terms of scientific research, he has won two invention patents, 10 utility model patents, and more than 30 software copyrights, and published more than 10 papers. His research domains include robot control system, machine learning, and image processing.
(156247874@qq.com)

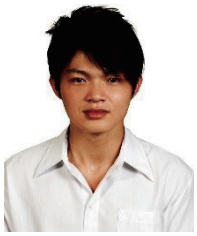

Che-Wen Chen received his B.S. degree from the Industry Engineering Management Department, Yuan Ze University, Taoyuan, Taiwan, in 2008, his M.S. degree from the Department of Civil Engineering, National Cheng Kung University, Tainan, Taiwan, in 2012, and his Ph.D. degree from the Department of Electrical Engineering, National Cheng Kung University, Tainan, Taiwan, in 2020. His current research interests include deep learning, NLP, robotics, and data science. (kfcmax300@gmail.com)

Shih-Pang Tseng received his B.S. and M.S. degrees from the Department of Electrical Engineering, National Cheng Kung University, Tainan, Taiwan, and his Ph.D. degree from the Department of Computer Science Engineering, National Sun Yat-sen University, Kaohsiung, Taiwan. He is a professor in Changzhou College of Information Technology. His current research interests include deep learning, NLP, robotics, and learning technology.
(tsengshihpang@ccit.js.cn)